THE UNIVERSITY *of* EDINBURGH

Edinburgh Research Explorer

Authigenic illite within northern and central North Sea oilfield sandstones: evidence for post-growth alteration

OPEN ACCESS

Authigenic illite within northern and central North Sea oilfield sandstones: evidence for post-growth alteration

M. WILKINSON[1],*, R. S. HASZELDINE[1] AND A. E. FALLICK[2]

[1] *School of GeoSciences, The University of Edinburgh, Grant Institute, The King's Buildings, West Mains Road. Edinburgh EH9 3JW, UK, and* [2] *Scottish Universities Environmental Research Centre, East Kilbride G75 0QF, UK*

ABSTRACT: It has been previously reported that late diagenetic fibrous illite, separated out from oilfield sandstones for dating by the K-Ar method, has systematically shown an increasing K-content with burial depth in the UK northern and central North Sea. This is surprising as fibrous illite is believed to form rapidly, in response to a geological event such as oil charging, and to retain its composition during subsequent burial. If the composition of the illite is related to present-day conditions, rather than the conditions of initial formation, then argon loss may have occurred, making K-Ar ages of questionable validity. Variations in crystal chemistry of the illite and their fundamental particle size and shape (length/width) distribution suggest alteration of the illite from the time of formation. The extent to which K-Ar ages of illite might need to be re-interpreted as a result of this post-formation alteration is not quantifiable at present; however there is evidence to suggest that the ages may be interpreted in terms of burial models involving both crystal nucleation and growth, and that a high proportion of Ar within the crystals may be retained during post-growth recrystallization.

KEYWORDS: authigenic illite, K-Ar age data, fundamental particle, North Sea, diagenesis.

Late diagenetic illite with a characteristic fibrous morphology is a common component of deeply buried sandstones. Although it is often only a minor component volumetrically, it has been widely studied for two reasons. Firstly, illite can be directly dated using the K-Ar technique, and there is considerable evidence that the age of the illite corresponds to the age of oil migration into a sandstone (Wilkinson *et al.*, 2006). Secondly, a relatively small volume of illite can reduce sandstone permeability by several orders of magnitude, making oil extraction difficult or impossible. Late diagenetic illite from North Sea

reservoir sands shows an approximately linear increase in potassium content with increasing burial depth, from ~4 wt.% at 2500 m depth to ~6.5% at 5000 m depth (Wilkinson *et al.*, 2006), but the trend remains unexplained. The correlation of composition and depth could be interpreted as evidence that the composition of the illite is related to the present-day burial conditions (temperature or porewater chemistry). Assuming that any recrystallization implies a loss of radiogenic argon from the illite crystals, and that any newly grown illite would have a relatively young age, then K-Ar ages would be at least partly reset. In this paper it is assumed that late diagenetic fibrous illite in oilfield sandstones of the northern and central North Sea formed initially coincidentally with a geological event such as oil charging (Hamilton *et al.*, 1989), the release of overpressure (Darby *et al.*, 1997), or

* E-mail: mark.wilkinson@ed.ac.uk

a tectonic / thermal event (Liewig & Clauer, 2000). The formation of the illite was controlled by nucleation processes, after which growth was rapid, leading to the fibrous morphology (Wilkinson & Haszeldine, 2002a). Here we investigate if there were subsequent, slower, processes leading to a long-term change in the illite chemistry, crystal size, or indeed, the K-Ar age. The nature of any subsequent processes such as recrystallization are investigated.

The potassium content of illite data utilized here are from the literature; they are all from late diagenetic fibrous illite samples separated from Jurassic hydrocarbon field reservoir sandstones from the northern and central North Sea (Brent Group: Glasmann *et al.*, 1989; Hamilton *et al.*, 1992; Hogg *et al.*, 1993; Mathews *et al.*, 1994; Girard *et al.*, 2002; Piper sandstone: Burley & Flisch 1989; Fulmar Formation: Darby *et al.*, 1997; Wilkinson *et al.*, 2006). The data set of Burley & Flisch (1989) also includes illite from shales interbedded with the reservoir sandstones. New data are presented from two boreholes that penetrate the Jurassic Fulmar Formation of the central North Sea, the K-Ar ages of which have been previously reported (borehole 29/10-2, Darby *et al.*, 1997, and borehole 29/5b-6, Wilkinson *et al.*, 2006; Fig. 1). The geological history and diagenesis of the Fulmar Formation in borehole 29/10-2 has been described in Wilkinson *et al.* (1994) and

Wilkinson & Haszeldine (2011), while borehole 29/5b-6 is from the Franklin Field described by Lasocki *et al.* (1999). All these data were originally collected for K-Ar age determination, and as such the illite samples were treated chemically to remove impurities such as Fe-oxides and carbonates. The physical separation of illite from other phases such as potassium feldspar was achieved by taking only the clay-sized fraction of the rock. The resulting samples are assumed to be 'pure' illite provided that contaminants were not detected using X-ray diffraction and transmission electron microscope imaging. In some studies residual K-feldspar could be detected (e.g. Burley & Flisch 1989). The possible detrimental effect of K-rich impurities on the reliability of K-Ar ages has long been recognized (Hamilton *et al.*, 1989).

METHODS

Sedimented aggregates of the illite separates were analysed by X-ray diffraction (XRD) to identify any major contaminants. Samples of illite were imaged using a transmission electron microscope (TEM), at 1:10,000–1:40,000 magnification. The dimensions of individual crystals were measured using a ruler on micrographs enlarged to approximately A4 dimensions, where the individual crystals were sufficiently separated to enable both long and short dimension to be determined. All particles
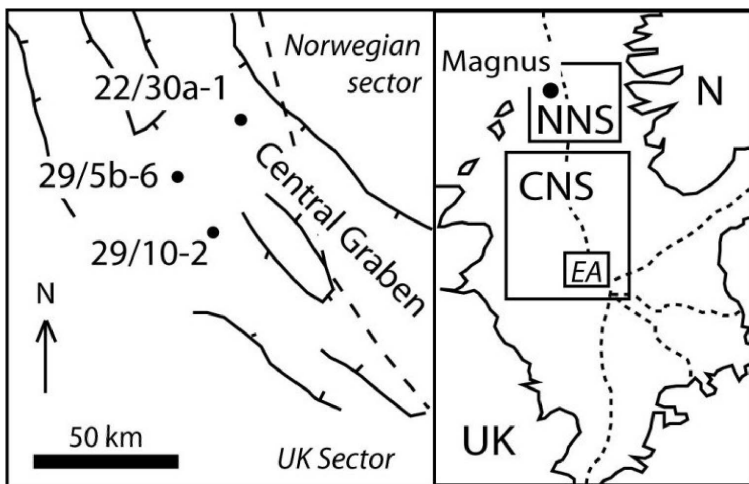

FIG. 1. Location map showing the oilfield boreholes for which illite particle size and compositional data are available, and the Magnus oilfield. NNS = Northern North Sea; CNS = Central North Sea; N = Norway; EA = enlarged area (on left).

which were sufficiently visible for a measurement to be made were measured – there was no other selection of particles. Between 18 and 107 crystals were measured in each photomicrograph, on 14 photomicrographs (Table 1). Measurements were almost all undertaken on photomicrographs of unshadowed samples, as the transparency of the very thin crystals allowed crystal edges to be viewed even where overlain by another crystal. This was not possible on shadowed photomicrographs, as the shadowing process renders the samples opaque. Particle thickness was measured on micrographs of samples that had been shadowed using platinum, with a shadowing angle of 1:4. Again, data were collected from all the possible crystals without selection, on 12–114 crystals per photomicrograph on 7 photomicrographs (Table 1). The chemical composition of 7 illite separates was determined using the methods of Neuman & Brown (1987; Table 2). Structural water contents of illites separates were assembled from literature sources and from previously unpublished data (Table 3).

RESULTS

The TEM photomicrographs show that the samples are dominated by illite, confirmed by both selected area electron diffraction, and by XRD of oriented samples. Occasional chlorite crystals, identified by stronger contrast fringe effects, were observed in sample 4237m from borehole 29/10-2. The amount of chlorite was not quantified in this sample, but was estimated from XRD analysis to be ~5% in sample 4356m from the same borehole (W.J. McHardy, pers. comm., 2 March 1993). The vast majority of the illite crystals appear to be euhedral within the resolution of the TEM, and of approximately hexagonal shape perpendicular to the presumed $c*$ axis (Fig. 2). Some more complex (but still euhedral) shapes were observed, and some samples contained a notably higher proportion of these complex shapes than others. Only a minimal number of crystals with anhedral boundaries were observed, which were interpreted as damaged, most probably during the extraction process. A single exception (negative 15498, borehole 29/10-2, depth 13901′) was observed to have a large number of irregular smaller crystals suggestive of dissolution. Irregular crystals were excluded from the size analysis if the damage was such that the original dimensions of the crystal could not be determined unambiguously. Photomicrographs were chosen so
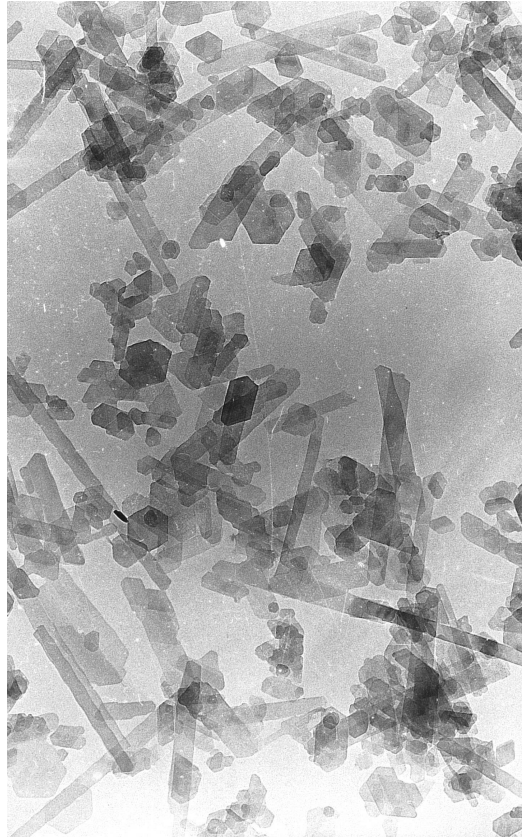
FIG. 2. Transmission electron micrographs of illite separated for K-Ar age dating. Field of view = 2700 nm; borehole 29/10-2, drillers' depth 4356 m.

that the separation of individual crystals was generally good, with few thick 'clusters' of crystals. Individual crystals vary from equant to lath-like, with axis dimensions of 22–3550 nm and short-axis dimensions of 15–731 nm. Borehole 29/10-2 has a unimodal distribution of crystal aspect ratio (mean length/width = 4.6±0.3), while borehole 29/5b-6 has a bimodal distribution with modes of length/width of ~2 and 5–6 (Fig. 3). The crystals of borehole 29/5b-6 have larger mean dimensions than those of borehole 29/10-2 (mean of maximum dimension: 430±20 nm, n = 394 and 300±17 nm, n = 346, respectively). The thicknesses of crystals in borehole 29/10-2 vary from 3–40 nm, with a mean of 13.8±0.6 nm.

TABLE 1. Dimensions of illite crystals.

Borehole	Core depth (ft)	Core depth (m)	Grain size (μm)	Photomicrograph numbers	Mean thickness (SE, n) nm	Mean length (SE, n) nm	Mean width (SE, n) nm
29/10-2*	13901	4237	<0.1	15498 15500 15502 15503	16.4 (1.3, 35) 11.3 (1.6, 12) 16.1 (1.1, 57)	469 (58, 62)	106 (14, 62)
	13999	4267	<0.1	15520		382 (62, 40)	114 (10, 40)
	14290	4356	<0.1	15480		297 (26, 107)	92 (7.1, 107)
				15482 15483 15484	9.6 (4.0, 5) 11.9 (1.8, 17) 12.9 (1.6, 15) 8.5 (1.0, 21)	340 (62, 18)	81 (12, 18)
				15485 15487		189 (20, 73) 204 (31, 49)	63 (3.8, 73) 64 (5.9, 49)
Mean for borehole 29/10-2					13.8 (0.6, 162)	304 (17, 349)	86 (4, 349)
29/5b-6[†]	17316	5278	<0.1	15814 15815		263 (28, 49) 352 (27, 73)	73 (8.3, 49) 87 (9.4, 73)
	17718	5400	0.05–0.1	15787 15793		606 (86, 41) 560 (57, 47)	122 (16, 41) 94 (14, 47)
	17734	5405	0.05–0.1	15772 15776		354 (41, 34) 397 (35, 74)	122 (19, 34) 144 (17, 74)
	17750	5410	0.05–0.1	15806 15809		512 (68, 45) 520 (107, 34)	82 (6.7, 45) 75 (7.0, 34)
Mean for borehole 29/5b-6						433 (20, 397)	101 (5, 397)
Magnus[‡]	~3000				3.13 (0.4, 22)	748 (94, 22)	145 (32, 22)

K-Ar age in: * Darby *et al.* (1997); [†] Wilkinson *et al.* (2006); [‡] data from Nadeau (1985).
SE = standard error; n = no. of measurements.

TABLE 2. Chemical analyses of illite separates.

Borehole	Depth (m)	Al_2O_3	K_2O	Na_2O	Fe_2O_3	MnO	CaO	MgO
22/30a-1	4650	21.2	7.9	0.1	1.4	0.0	0.3	1.6
	4654	24.4	7.5	0.1	1.5	0.0	0.3	1.5
	4657	23.4	8.4	0.2	1.6	0.0	0.4	1.3
29/10-2	4199	22.7	7.5	0.2	2.9	0.0	0.8	2.6
	4199	25.2	7.7	0.1	2.4	0.0	0.3	2.6
	4221	25.7	7.6	0.1	2.2	0.0	0.2	2.4
	4356	26.4	7.7	0.1	2.4	0.0	0.4	2.2
	4199	26.4	7.3	0.1	2.5	0.0	0.8	2.3

DISCUSSION

Data quality − contamination of illite samples with detrital material

Contamination of illite separates with detrital K-bearing minerals (muscovite, K-feldspar, mixed layer illite-smectite) is an acknowledged problem with the K-Ar method used to date authigenic illite (e.g. Glasmann *et al.*, 1989). To quantify any such contamination, K-Ar ages were plotted against K_2O content on the assumption that any detrital mineral would be significantly older than the authigenic illite (at least 160 Ma for the Brent Group). Figure 4 shows to some degree a positive correlation between K-Ar age and K-content, the oldest end-member with low-K content − this is

unexpected as both muscovite and K-feldspar have higher K contents than authigenic ilite. However, it is apparent that only three of the data sets demonstrate this correlation − both the sandstones and shales of Burley & Flisch (1989), and Glasmann *et al.* (1989), while the data of Hamilton *et al.* (1989) show a weak positive correlation which is discussed below in the context of a two-end-member model for authigenic illite composition. In the remaining data there is no visible correlation between K-Ar age and K-content. Both Burley & Flisch (1989) and Glasmann *et al.* (1989) suspected that their illite separates were contaminated with detrital material, and both authors attempted to correct their measured ages for the effects of contamination.
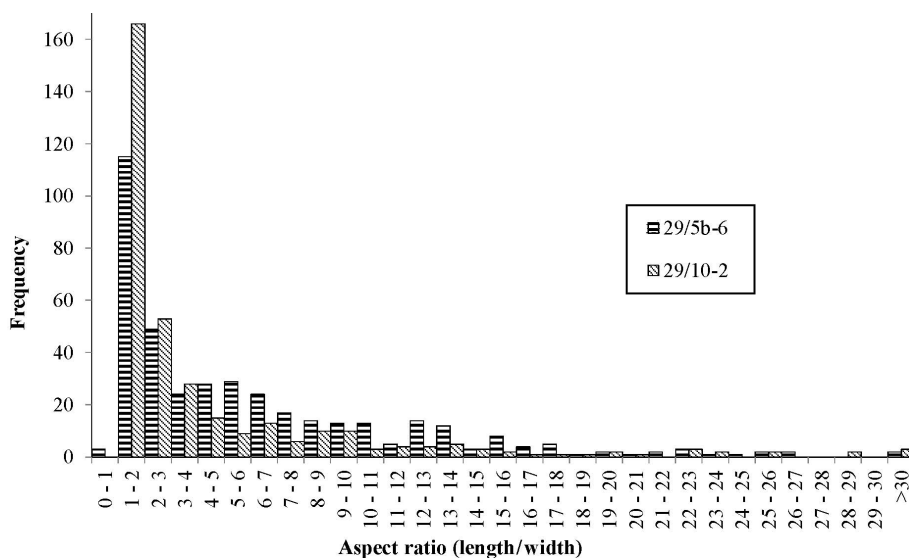

FIG. 3. Crystal aspect ratio (length/width) for boreholes 29/10-2 and 29/5b-6.

TABLE 3. Structural water contents of illites.

Well	Core depth (m)	Grain size (μm)	Water μmoles/mg
9/8a-9*	3999	<0.16	3.3
9/8a-10*	3911	<0.2	5.0
9/9b-4*	3780	<0.16	3.2
	3903	<0.2	3.6
9/9b-9*	3600	<0.2	3.0
	3517	<0.2	6.2
9/9a-11*	3927	<0.1	3.1
9/9a-13z*	3843	<0.5	4.7
	3843	<0.1	5.3
	3843	<0.2	5.2
9/9a-14*	4659	<0.5	3.9
	4683	<0.1	3.0
	4703	<0.5	3.0
22/30a-1	4650	<0.1	2.8
	4654	<0.1	2.7
	4657	<0.1	2.5
	4663	<0.1	3.4
	4664	<0.1	2.6
	4667	<0.1	2.4
23/27-6	3895	<0.1	2.1
	3871	<0.1	2.1
	3902	<0.1	1.9
29/10-2[†]	4199	<0.1	3.0
	4199	<0.1	2.6
	4199	<0.1	3.1
	4221	<0.1	2.8
	4237	0.1−0.0 5	2.8
	4267	<0.1	3.1
	4267	<0.1	3.0
	4298	<0.1	3.8
	4298	<1.0–0.1	2.7
	4356	<0.1	3.7
	4356	<0.1	2.8
30/17b-5	4117	<0.1	2.0
	4117	<0.1	3.0
211/12-1[‡]	2938	<0.1	2.2
	2938	0.1–0.5	2.5
	2946	0.1–0.5	3.8
	2963	<0.1	2.8
	2963	0.1–0.5	2.6
	2963	0.5−1.0	2.7
	2976	<0.1	2.7
	2976	0.1–0.5	3.0
	2984	0.1–0.5	2.9
	2984	0.5−1.0	3.4
211/12a-M1[‡]	2937	<0.1	2.7
	2937	0.1–0.5	2.6
	2993	<0.1	2.8
	2996	0.1–0.5	2.9
	3043	<0.1	3.2
	3043	0.1–0.5	3.5
	3064	0.1–0.5	3.6
	3185	0.1−0.5	3.2
16/8a-4[§]	4747	1−2	2.4
16/8a-4[§]	4747	1−2	2.4
16/8a-4[§]	4783	1−2	2.0

* McBride (1992). [†] $\delta^{18}O$ and δD in Wilkinson et al. (1994), H_2O yield previously unpublished. [‡] $\delta^{18}O$ in Fallick et al. (1993), H_2O yield previously unpublished. [§] Greenwood et al. (1994).

In both cases these corrections produced younger ages for the authigenic component as the contaminant was assumed to be older, indeed measured as older in the case of the data of Burley & Flisch (1989). In both studies the contaminants were assumed to be small percentages of muscovite or K-feldspar that were sufficiently abundant to be detectable by X-ray diffraction in some samples. However, as above, both K-feldspar and muscovite contain more K than the authigenic illite being discussed here – consequently it is not possible to account for the correlation in Fig. 4 by this mechanism. Contamination by a K-free phase such as quartz should have no effect on the K-Ar age and can also be eliminated as a cause. Simple modelling of K and Ar contents of physical mixtures of illite and a contaminant shows that the detrital material in the illite mixtures must be both significantly older than the depositional age of the sediments and have a low K content. An age range of 425−3350 Ma was used from the ages of detrital zircons in the northern North Sea (Morton *et al.*, 2009), suggesting K_2O contents of ~0.1−1.5% and contamination levels of 30−50%. The only likely material is detrital smectite or I/S, which is confirmed by Burley & Flisch (1989) who recorded

I/S expandability of up to 50%. Figure 4 also shows that the contamination can be largely negated by eliminating all samples with ages greater than 80 Ma; this procedure is adopted here henceforth.

The plot of K_2O *vs.* depth for samples with a K-Ar age of less than 80 Ma, i.e. free from detectable detrital contamination as above, has a correlation coefficient (R^2) of 0.43, which for 119 points is significant at any reasonable degree of confidence (Fig. 5). The trend of increasing K-content with depth within authigenic illite reported by Wilkinson *et al.* (2006) hence appears to be robust despite probable detrital contamination within some of the data originally reported.

Controls on illite K-content

TEM analyses have shown that the fibrous illite has a complex crystal structure, whereby a 'single' crystal is composed of a stack of crystallites termed fundamental particles (Nadeau, 1985; Kang *et al.*, 2012). A possible explanation of the change in illite composition with depth is that the fundamental particles within the illite fibres continue to thicken after the period of initial growth. According to the fundamental particle theory, each illite particle
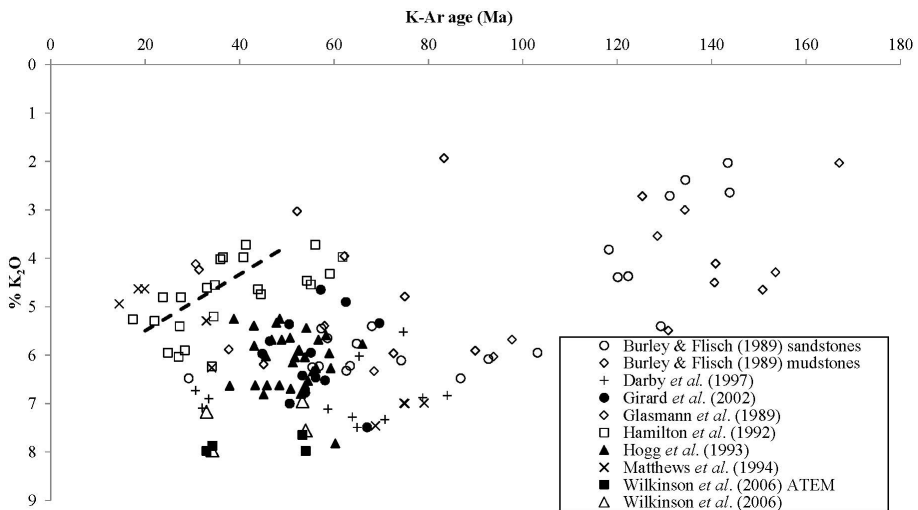

FIG. 4. K-Ar age *vs.* K-content, showing a loose positive correlation here interpreted to be the result of contamination with either detrital smectite or I/S. Note that there is no evidence of significant contamination in samples with measured ages less than 80 Ma., The data of Hamilton *et al.* (1989) show a weak positive correlation between K-Ar age and K-content, with a possible mixing line between 2 illite sub-populations marked as a dashed line.
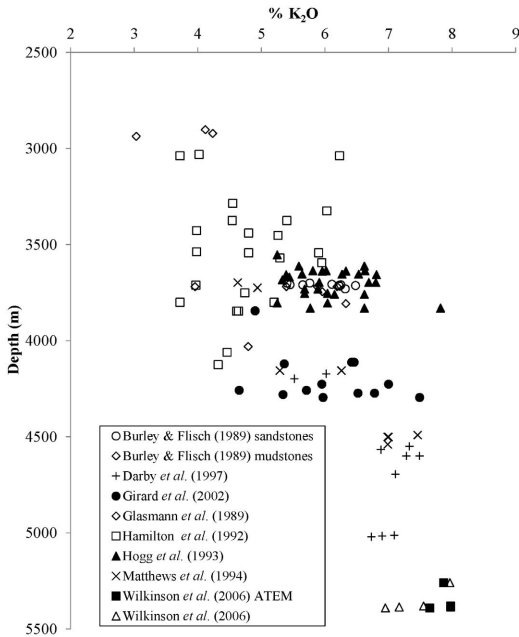
FIG. 5. Measured K_2O of illite samples free from significant detrital contamination (<80 Ma old, see text) *vs.* present-day burial depth. The correlation is significant at any reasonable level of confidence.

consists of alumino-silicate layers joined by non-expandable K-rich layers with a minimum thickness of 2 nm, separated by interfaces that give the mineral expandable properties; see Kang *et al.* (2012). Figure 6 compares whole-illite chemical analyses (Table 2) with the calculated composition of illite in borehole 29/10-2 at 4237−4356 m burial depth for different fundamental particle thicknesses using the model of Yates & Rosenberg (1998). The model assumes 'ideal' illite, with no atomic substitution for either the cation or anion sites. The analyses of the illite (Table 2) show both Fe and Mg, which substitute for Al in a solid solution with the mineral phengite (Deer *et al.*, 1966). The analytical Al-contents can be corrected to allow for this (Fig. 6); the corrected data lie on the high-Al side of the Yates & Rosenberg (1998) correlation, while the uncorrected data lie on the low-Al side. The data hence bracket the model compositions, suggesting that the analysed illite is composed of fundamental particles with an average thickness of 2−4 alumino-silicate layers correspond to a mean fundamental particle thickness of 2−4 nm. Such thicknesses have been measured for illite fundamental particles from the northern North Sea: in an unidentified borehole in the Brent Group (Rannoch Formation) authigenic illite has an average particle thickness of 3.7 (±1.4) nm, and in the Magnus
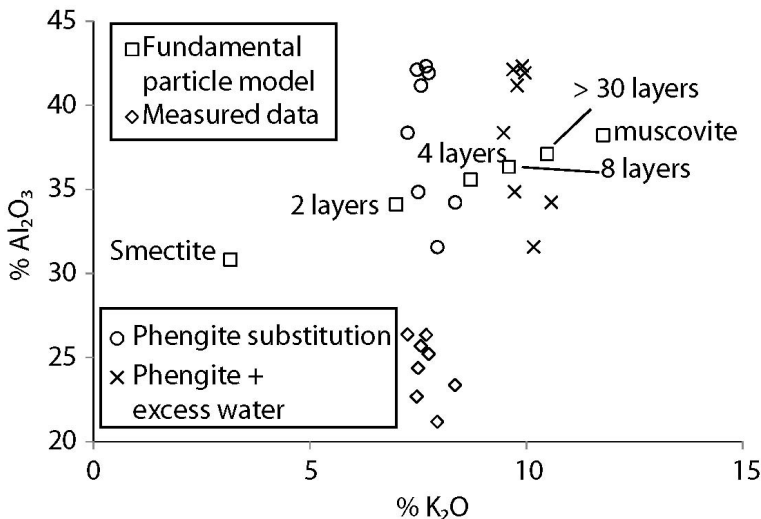

FIG. 6. Whole-illite analyses and the calculated composition of illite for different fundamental particle thicknesses using the model of Yates & Rosenberg (1998). Analytical data are plotted as measured, with Al-contents corrected for the phengite substitution, and with K-contents corrected for excess structural water as hydronium in the octahedral layer.

Sandstone an average of 3.1 (±1.8) nm (Nadeau, 1985). However, measured thicknesses (sample averages) of 8.5 to 16.4 nm were determined for samples from borehole 29/10-2 in this study (Table 1). Clearly there is a discrepancy; either the illite crystals are individual fundamental particles that are thicker than suggested by the Yates & Rosenberg (1998) model (8 or more illite layers) or the crystals visible in the TEM photomicrographs are not individual fundamental particles, but are each composed of multiple stacks of fundamental particles, in layers two or more fundamental particles thick. Given the euhedral nature of the crystals imaged in this study, and the lack of evidence for differing thicknesses of individual crystals (the crystals are partly transparent to electrons, allowing overlapping crystals or steps in crystal thickness to be clearly seen on the TEM photomicrographs), then it is concluded that the imaged crystals are single fundamental particles.

A preferred explanation for the discrepancy between the measured K contents and the model of Yates & Rosenberg (1998) is that there are cations other than K in the interlayer sites: H_3O^+, NH_4^+ and Na are all possibilities. Chemical analyses (Table 2) show significant Mg, and Fe, and lesser Na. Hydronium (H_3O^+) is also a possibility; a compilation of illite water contents analysed at SUERC frequently have excess structural water compared to the structural formula (Table 3; Fig. 7), with an average of 3.1±0.1 μM/mg (1 standard error, n = 56) compared to 2.5 to 2.7 μM/mg from the structural formulae of Yates & Rosenberg (1998). The data were measured on samples with a single pre-treatment method (overnight de-gassing *in vacuo* at 120ºC); dehydroxylation procedure (*in vacuo* heating to ~1200ºC in a platinum crucible); and measurement method (manometry of released hydrogen). However, the samples were likely to be of variable purity, and kaolin (a possible contaminant) has significantly higher water content than illite at ~8 μM/mg and smectite, the most probable contaminant (see above) at ~5 μM/mg. Given the recorded water contents in the illite separates, then up to 70% kaolin would be required in the illite, an unlikely level of contamination.

Figure 6 shows the measured illite compositions with 3% hydronium added to the interlayer site, suggesting a fundamental particle thickness of ~8 nm, or greater. This reconciles the calculated and measured particle thicknesses, and is consistent with the imaged illite crystals being individual fundamental particles rather than composites. There is no significant trend of illite water content and present-day burial depth, and insufficient data to test the hypothesis that there is variation with the original depth or temperature of crystallization. However, we note that a distinct difference in structural water was noted between fields on the shelf and those in basins for illites from the southern North Sea (Ziegler *et al.*, 1994), where depth of formation is at least one of the potential controlling variables. Note that Jiang *et al.* (1994) claimed that hydronium cannot significantly occupy the interlayer site in illite, and that Matthews *et al.* (1994) attributed measured low-K contents to undetected quantities of smectite, kaolin and/or quartz in the illite separates. In contrast, Drits & McCarty (2010) interpret thermogravimetric analysis data as demonstrating water in K-sites in illite, and detailed analyses of interlayer cations in the Silver Hill illite, Montana, support a structural model in which hydronium partly replaces potassium (Nieto *et al.*, 2010). Whether the excess water
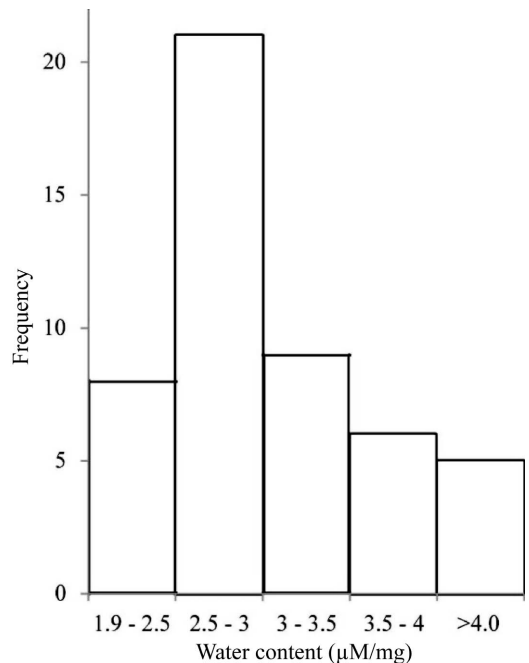

FIG. 7. Illite commonly has excess structural water compared to 2.5 to 2.7 μM/mg for the fundamental particle model of Yates & Rosenberg (1998). Determined during measurement of δD; data sources in Table 3.

is hydronium (H_3O^+) or water (H_2O) has been debated (Vidal *et al.*, 2010) but is not important for the purposes of the present discussion.

As well as the fundamental particle model, there are other models to potentially explain the correlation between K-content and burial depth in illite. Firstly, the K-content could be determined by a temperature-dependant distribution coefficient between illite and the porewater, which determines how much hydronium is incorporated into the structure. As temperature increases, the change in the distribution coefficient could cause less hydronium (and hence more K) to be taken into any newly-formed illite. Primmer *et al.* (1993) showed a phase diagram illustrating that high-K illite is favoured by high K/H in porewaters, while Aja (1995) reported that the solubility of natural illite was controlled by mica-like phases with variable K-contents, which could be taken to support the principle of variable distribution coefficients. Alternatively, even if the distribution coefficient has little or no temperature dependence (in the

relevant temperature range) then if the K-concentration of porewaters increases with depth, then any later (younger) illite might be expected to have higher K contents. Figure 8 shows porewater analyses from Jurassic oilfield sandstones of the UK northern and central North Sea for the depth range of 2.8−5.5 km, the same range for which (uncontaminated) illite analyses are available. There is no increase in the concentration of K or K/H in porewaters with increasing burial depth in the UK northern North Sea but an increase, or at least an increase in the maximum values, in the UK central North Sea (data from Warren & Smalley, 1994). Porewaters in oilfield sandstones in the Norwegian sector of the North Sea show no changes (Egeberg & Aagaard, 1989); this area has geology which is closely related to the UK northern North Sea. Drawing firm conclusions from this exercise is limited by the data availability. The depth ranges of the two porewater composition data sets are not the same − the central North Sea data includes significantly more data from deeper than 3.5 km,
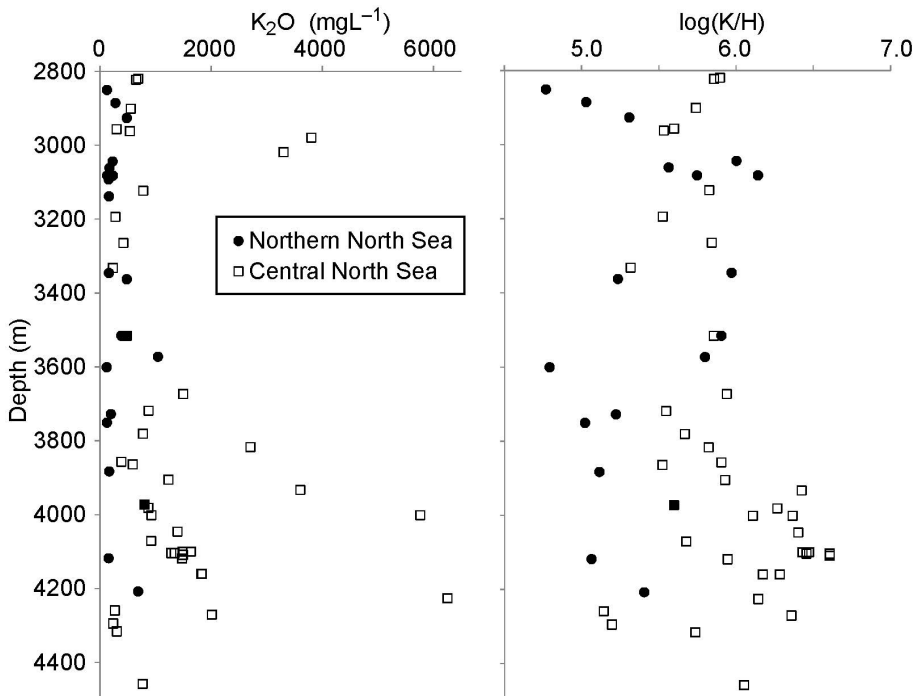

FIG. 8. Porewater K_2O and log(K_2O/H) for the Jurassic oilfield sandstones of the northern and central North Sea versus burial depth (data from Warren & Smalley, 1994) for the same depth range for which illite compositional data are available. There is no significant change in K_2O or K_2O/H in the northern North Sea, but an increase in the maximum values of both K_2O and K_2O/H in the central North Sea with increasing burial depth.

where K and K/H are highest. Where significant data are available for both areas, the data show considerable overlap. Nevertheless, the porewaters of the central North Sea appear to have higher concentrations of K at depths greater than ~3800 m. It is also conceivable that the $K^+:H_3O^+$ ratio of the illite undergoes dynamic alteration on a geological timescale, with post-growth alteration by solid-state diffusion within the fundamental particles which are of nanometre scale-thickness. In this case, the $K^+:H_3O^+$ ratio would increase in response to either higher temperatures (and hence altered distribution coefficient) or higher K concentrations in porewaters, but without new growth or recrystallization of the illite. It is therefore impossible to draw a firm conclusion as to whether any increase in K-content of illite with depth (that is not due to thickening of the fundamental particles; see below) is controlled by changes in the K concentration in porewater, or by a temperature-dependent distribution coefficient, and whether or not new growth or recrystallization is required.

Origin of the K-depth correlation − mixing of 2 geographical populations

The data in Fig. 5 are from two adjoining geographical areas, the central and northern North Sea (Fig. 1). It is possible that the correlation between K-content and burial depth of illite is an artefact of two illite populations at different depths in the two geographical areas. As the porewaters in the deeper parts of the central North Sea have significantly higher K concentrations (Fig. 8), then illite with a higher K-content might be expected here, assuming that the K-content is indeed partly controlled by a distribution coefficient, with the remaining interlayer sites occupied by hydronium. The central North Sea samples have a range of burial depths that is deeper than the range for the samples from the northern North Sea, hence the K-content depth correlation could be an artefact of the two populations. Figure 9 shows K-content *vs.* depth for the <80 Ma old illite, split into the two geographical areas. Although the illite samples are from different depth ranges, they have similar best-fit lines, and both correlations are significant at any reasonable degree of confidence. It is concluded that the correlation between K-content and burial depth is not an artefact of the mixing of two geographical illite populations, but that there is a

genuine increase in K-content of illite with burial depth that is common to both the central and the northern North Sea.

Origin of the K-depth correlation − present day or palaeo-depth?

The correlation of K_2O content of illite versus burial depth (Fig. 5) uses the present-day depth. However, given that the illites are dated as growing between 14 and 80 Ma ago, they clearly formed at some other burial depth. The study area has had a relatively simple burial history since ~100 Ma ago of effectively continuous subsidence without
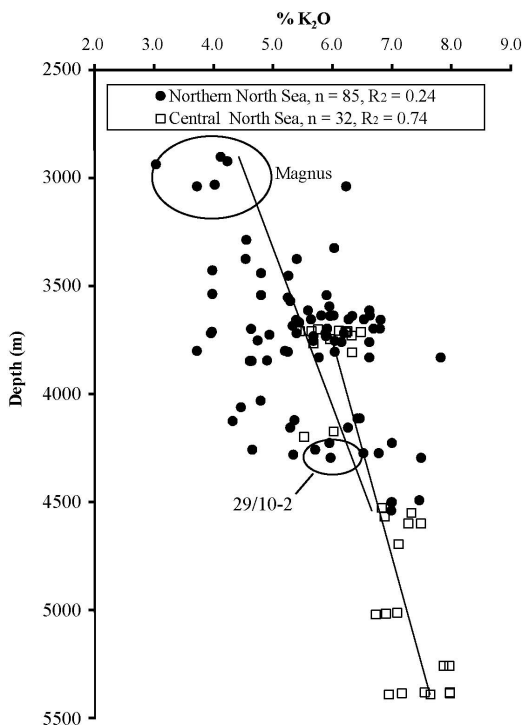

FIG. 9. Illite K-content *vs.* burial depth for the two geographical areas, the northern and central North Sea. Note that although the illite samples are from different depth ranges, they have similar best-fit lines, and both are significant at any reasonable degree of significance. It is concluded that the correlation between K-content and burial depth is not an artefact of the mixing of two geographical illite populations. Also shown are the illite compositions for the Magnus Field and borehole 29/10-2 predicted from the fundamental particle model using the measured particle thickness and allowing for hydronium and other cation substitution, see text.

significant uplift. Given that the age of each illite sample is known, it is possible to correct each present-day burial depth back to the time of illite growth using burial curves presented with the published data. It should be noted that the published burial curves are not very precise, and are frequently hand-drawn through a minimal number of data points. Neither are the majority corrected for the compaction of the sediments during burial, though this is probably a secondary source of error. It is clear that the restored depths are at best only accurate to plus/minus a few hundred metres, perhaps even 500 m where burial is rapid. Ages earlier than ~100 Ma would be difficult to correct for, as the burial curves include unconformities with possible erosional episodes of unknown severity (from borehole logs released by the UK Government). However, as illite with age dates of older than 80 Ma have been omitted due to suspected contamination (see above), this is not of concern here.

The plot of apparent formation depth versus potassium content of illite has a correlation coefficient (R^2) of 0.02, which is not significant at any reasonable level of confidence (Fig. 10). Two conclusions can be drawn from this: firstly there was no significant systematic variation in K-content at the time of illite formation; and secondly that the correlation between present-day depth is either entirely coincidental, or is the product of processes such as recrystallization acting after the initial growth of the illite. If the latter is the case, then it is entirely possible that the post-growth process has altered the K-Ar age in some way, most likely by adding new (young) illite or by allowing argon to escape during recrystallization. In both cases the measured age would be younger than the original growth age. In either event, the depth correction used to produce Fig. 10 would be questionable. Evidence for the processes acting on the illite after the initial period of growth are discussed below.

The plot of inferred burial depths of formation of the illite implies low temperatures of illite growth; assuming a palaeo-thermal gradient of 35°C/km and a generous sea-floor temperature of 15°C, then growth temperatures of 15−50°C are implied. While some authors have accepted that illite may grow at such temperatures (e.g. Darby et al., 1997; Lander & Bonnell, 2010), others place illite growth at much higher temperatures, frequently in excess of 100°C (e.g. Ehrenberg & Nadeau, 1989).

Proposing that much of the illite in the North Sea grew at low (<50°C) temperatures conflicts with petrographic evidence; for example the low abundance of illite (especially the pore-filling fibrous morphology type) in shallow buried, low-temperature (~2 km; 70−80°C) sandstones at the present day in the North Sea (e.g. Giles et al., 1992).

Origin of the K-depth correlation − physical mixing of two end-member illites

One of the simplest mechanisms to produce a correlation involving composition is a mixing line between two end-members, with each end-member of approximately fixed composition. The correlation between K-content and burial depth would then be the product of a mixing between a relatively low-temperature illite with low K content and a higher temperature illite with a higher K content. In this scenario, the more deeply buried illites would contain a higher proportion of the higher tempera-ture, high-K end-member. Speculatively, the rela-tively low-temperature illite might be the result of a geological event early in the burial history of the sandstone, while the higher temperature illite
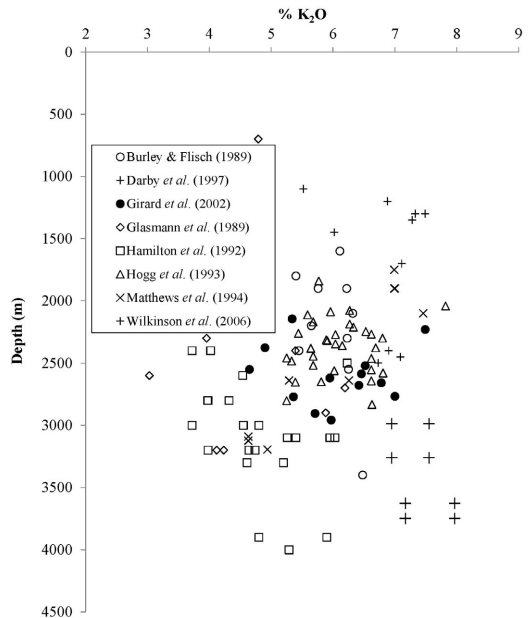

FIG. 10. Potassium content of illite vs. apparent formation depth. There is no correlation at any reasonable degree of significance.

represents recrystallization or later growth. The early event could be oil charging (Hamilton *et al.*, 1989), the release of overpressure (Darby *et al.*, 1997), or a tectonic/thermal event (Liewig & Clauer, 2000) and is probably not the cause of the very early grain-coating illite occasionally recorded from some North Sea sandstones that is discussed by Wilkinson *et al.* (2006, pp. 159−160). Certainly the intention of illite separation is to obtain the late diagenetic fibrous illite for age dating, though the extent to which any earlier illite has been eliminated is very difficult to assess. There is some evidence to support the mixing-line hypothesis: experimentally grown illite has been shown to have a bimodal distribution of K-contents (average K atoms per unit cell 1.1 and 1.7; Primmer *et al.*, 1993) which exceeds the analytical error of the TEM method (0.3 atoms per unit cell). Diagenetic fibrous illite from the Permian Rotliegendes sandstones, UK southern North Sea also has bimodal K-contents (Leveille *et al.*, 1997). The data considered here have a distribution which is broadly normal with a mode at ~6% K_2O, but with a possible minor peak at 3.75−4% K_2O (Fig. 11). It

is apparent that there are insufficient data to draw a firm conclusion.

An alternative way of testing the mixing line hypothesis is by plotting K-Ar age *vs.* K_2O content, though this procedure has already been used to eliminate some of the data where contamination of the illite separates by detrital material was suspected, as above. The data with ages less than 80 Ma show no overall correlation between K-Ar age and K_2O content (Fig. 4); consequently there is no evidence for two or more generations of illite basin-wide, or else any such generations differ sufficiently between the assembled data sets that there is no regional pattern. However, the one data set that covers a large age range (Hamilton *et al.*, 1989; 15−63 Ma) shows a weak positive correlation between K-Ar age and K-content. Taking the end-member K_2O contents to be 3.75 and 5.5% (as above), then ages of 50 and 20 Ma would be predicted (Fig. 4). As expected, the younger illite is more K-rich, consistent with the regional increase in K-content with burial depth (Fig. 5). As above, one interpretation of such a mixing line is that the old illite end-member represents event-triggered illite precipitation, and
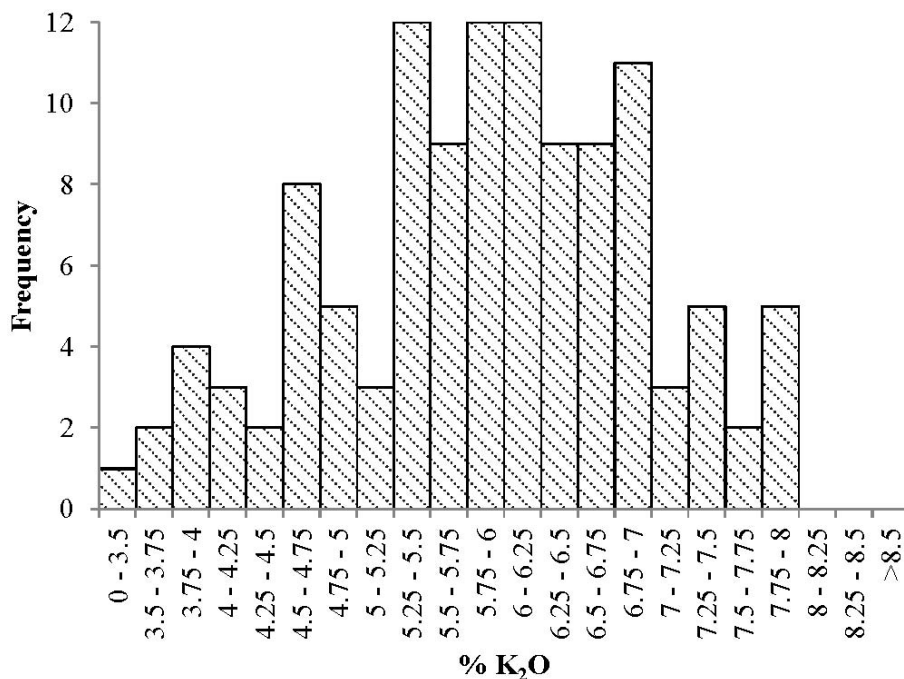

FIG. 11. Potassium (as %K_2O) for illite has a distribution which is broadly normal but with a possible minor peak at 3.75−4% K_2O. This is at best weak evidence for the existence of two illite populations that are physically mixed to produce the correlation seen in Fig. 5.

the younger end-member represents subsequent new growth or recrystallization.

Illite crystal morphology: Plates vs. laths

Transmission electron micrographs show that illite fundamental particles have two morphologies, here termed plates and laths after Bauer *et al.* (2000). A histogram of length/width of individual illite fundamental particles for borehole 29/5b-6 shows a bimodal distribution, defining plates and laths with a threshold value of length/width of ~3 (Fig. 3), as also reported by Lanson & Champion (1991) for fundamental particles probably extracted from shales at similar burial depths. It might be speculated that, if the correlation between K-Ar age and K_2O content is due to the physical mixing of two generations of illite, then the two generations could correspond to plates and laths. As acicular (fibrous) crystals are usually the result of rapid growth (Mullin, 1961) it might be imagined that the laths would preferentially form during an 'event' corresponding to high degrees of pore fluid supersaturation with respect to illite (Wilkinson & Haszeldine, 2002a), while the plates were the result of slower growth under lower degrees of super-saturation, and so might be younger than the laths. It is not inconceivable that the plates are derived from the early, grain coating illites occasionally observed in North Sea sandstones (described in Wilkinson *et al.*, 2006) but there is no obvious way of testing this hypothesis at present. The experimental growth of illite of Bauer *et al.* (2000) is broadly in agreement with this synthesis, except that Bauer *et al.* (2000) described the formation of the laths as 'slow'. Given that the laths were produced in a laboratory in 60−840 days, this seems to be a very rapid process indeed, from a geological perspective. There are insufficient data available to test the hypothesis that the plates and laths observed in diagenetic illite are of different ages or present at different burial depths, and hence it is not possible to test the hypothesis that the correlation between K_2O content of illite and burial depth might be a physical mixing line between plate and lath crystal morphologies.

Origin of the K-depth correlation − change in thickness of fundamental particles

As discussed above, the K-content of illite depends upon the thickness of the constituent

fundamental particles. Hence, the observed correlation between K-content of illite and depth could be a product of changing fundamental particle thickness, with the fundamental particles expected to become thicker with increasing temperature. Figure 12 shows the thickness of the fundamental particles from the study area, including the results of numerical modelling of illite nucleation and continuous (not episodic) growth by Lander & Bonnell (2010) in the Norwegian sector of the North Sea. Assuming present day temperatures for borehole 29/10-2 of ~160±5°C then it is clear that all the available measured data are a reasonable fit to the model. The model assumes continuous growth of illite crystals (i.e. continuous modification), and does not incorporate 'events' such as oil filling or overpressure release which have been claimed as the triggers for the precipitation of illite (Hamilton *et al.*, 1989; Darby *et al.*, 1997;
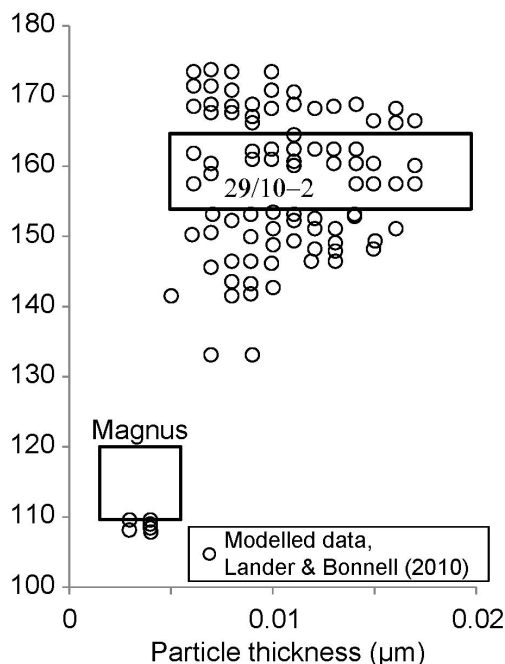

FIG. 12. Thickness of fundamental particles *vs.* present-day burial depth. There is good agreement between a theoretical model of the Norwegian sector of the North Sea (Lander & Bonnell, 2010) and the measured data, suggesting that the modelled processes (nucleation followed by continuous growth limited by solute availability) may be realistic. Magnus oilfield and borehole 29/10-2 are plotted as the mean ± 1 standard deviation.

Wilkinson *et al.*, 2006). Instead, the model has illite growth as a continuous process controlled by the availability of K, Al and Si, and of suitable surfaces for nucleation. Note however that there is a discrepancy between measured and modelled K-Ar ages for the model of Lander & Bonnell (2010), explained by these authors as due to contamination of the illite samples by geologically old muscovite or detrital K-feldspar. It seems to be within the bounds of possibility that illite nucleation is in many cases controlled by specific episodic geological events, but that the crystals continue to grow (and possibly also nucleate) in a manner described by the Lander & Bonnell (2010) model. The discrepancy between measured and modelled K-Ar ages in the Norwegian North Sea data using the Lander & Bonnell (2010) model might then be plausibly accounted for by these geological events upon nucleation.

It is also possible to restore the thickness data back to the depths of formation, using burial curves as above. The Magnus Field illite (burial curve and K-Ar age of 42−55 Ma from Macaulay *et al.*, 1992) would have grown at ~1700−2000 m depth, while the illite from borehole 29/10-2 would have grown at between 1200 and 1700 m. It is clear that the thinner illite fundamental particles from the Magnus Field would have grown at deeper burial depths, and hence almost certainly higher temperatures, than the thicker illites from borehole 29/10-2. While these are only effectively two data points, they support the hypothesis that the measured fundamental particle thickness is a function of present-day burial depth, and not of the depth (temperature) of putative formation. This is reasonable evidence of alteration of the illite after the initial growth stage, in this case by the thickening of the fundamental particles controlled by the present-day burial temperature.

Can the thickening fundamental particle model account for the correlation between illite K-content and present-day burial depth? Illite from the Magnus Field, approximate depth 3000 m, has a thickness of approximately 3 nm (Nadeau, 1987), corresponding to a theoretical K_2O content of between 7 and 8.7% (Yates & Rosenberg, 1998). Allowing for 1−0.7% water (3.1 µM/mg hydronium regional average, as above, minus 2.5 to 2.7 µM/mg from the model of Yates & Rosenburg, 1988) and ~3% other cations (Table 2), a measured K_2O content of 3 to 5% is predicted, while for the more deeply buried borehole 29/10-2 illites, a value

of ~5.5−6.5% is predicted (Fig. 9). This exercise produces a reasonable fit to the regional K-depth trend, giving some confidence in the model of thickening fundamental particles. Clearly, there are insufficient data for this exercise to be in any way conclusive, and is in any case approximate given the lack of compositional data for the Magnus illites.

A potential mechanism by which the thickening of the fundamental particles can occur is ripening, whereby the size distribution of a collection of crystals moves towards a larger size by the preferential dissolution of the smaller crystals. This mechanism has been identified as important in the genesis of hydrothermal mixed I/S (e.g. Eberl & Środoń, 1988). In theory, the ripening process leads to a characteristic distribution of crystal size distribution (Baronnet, 1982). Figure 13 shows data from boreholes 29/10-2 and 29/5b-6 against model curves for crystal growth controlled by diffusion, first order and second-order kinetics (Baronnet, 1982). There is a reasonable fit between the measured data and the model curve for second-order kinetics, but a significant mismatch between the data and diffusion or first-order kinetics. Given that the fibrous morphology of diagenetic illite has been interpreted as evidence of rapid, nucleation-limited growth (Wilkinson & Haszeldine, 2002a) then under such conditions (once growth has been initiated) the supply of nutrients to the crystal is the limiting process, i.e. diffusion. Hence, the expected result for fibrous crystals is that the thickness data should match the diffusion-limited curve, which they clearly do not. Instead, second-order growth takes place by spiral crystal growth under low-supersaturation conditions (Baronnet, 1982), which do not match the conditions required for the initial formation of fibrous illite. Spirals have been observed on the (001) surfaces of a tiny minority of the fundamental particles examined for this study; however the spirals are only one alumino-silicate layer thick (1 nm) and cannot be easily imaged at the magnifications used for this study. Other consequences of the ripening process are a change in the size distribution of particle size through time, towards broader, flatter distributions and higher mean values (Baronnet, 1982). It is not simple to test the available data against these predictions, as both time (since initial growth) and temperature (as the probable control on the rate of precipitation) need to be taken into account. The assumption would also have to be made that the
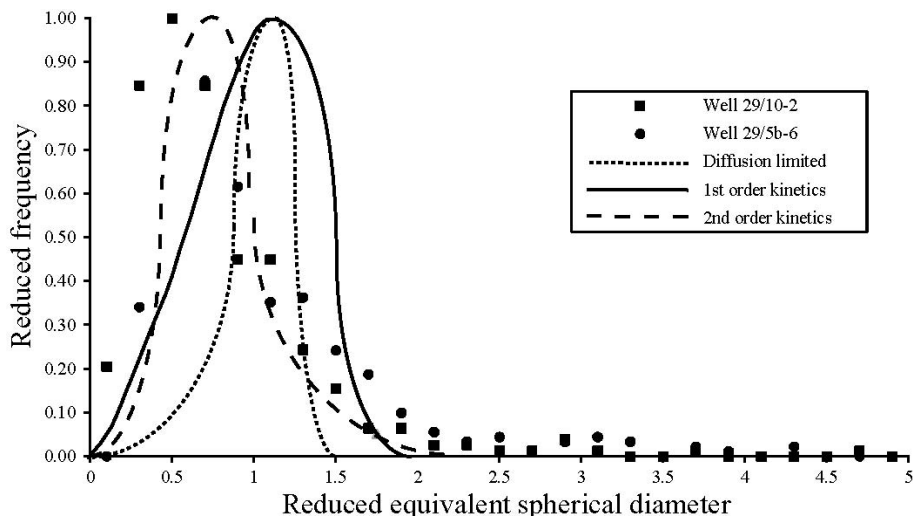
FIG. 13. Crystal size distribution for wells 29/10-2 and 29/5b-6 against model curves for crystal growth controlled by diffusion, first order and second-order kinetics (Baronnet, 1982). There is a reasonable fit between the measured data and the model curve for second-order kinetics, but a significant mismatch between the data and diffusion or first-order kinetics. Reduced equivalent spherical diameter (ESD) = ESD / mean ESD; reduced frequency (F) = F/maximum F.

illite formed with similar crystal size distributions, for which there is no evidence.

Significance for interpretation of K-Ar ages

We conclude that the size distribution of the fundamental particles provides evidence for the alteration of the size distributions of the illite fundamental particles by ripening, after the initial phase of nucleation and growth. This appears to disprove the hypothesis most commonly used to interpret K-Ar ages of illite, that the illite grows as a single geological event (e.g. related to oil filling or over-pressure release), and then remains entirely unaltered during subsequent burial. A possibility is that the composition of the illite changes, yet the age (i.e. the relative K and Ar contents) is at least partly preserved, a hypothesis suggested for the transformation of smectite to illite in mudrocks (Wilkinson & Haszeldine, 2002b). While the mechanisms of illite growth in sandstones and shales are quite probably different (Clauer *et al.*, 1999), it is interesting to note that modelling of the smectite to illite reaction in shales of the Texas Gulf coast (USA) suggested that between 75 and 100% of the argon within the smectite was retained by the newly formed illite. Certainly there has been no zero-age illite recorded within the North Sea

reservoir sandstones, as might be expected if the illite was constantly recrystallising during burial and consequently losing the retained argon. Given that the process of K-content change within the fibrous illite from oilfield sandstones is currently unknown, it is not possible to model the process and hence correct the measured K-Ar ages for any suspected loss of argon. Such correction may become possible in the future.

CONCLUSIONS

(1) Late diagenetic fibrous illite from the northern and central North Sea has a trend of increasing content of K_2O with present-day burial depth that is robust despite evidence for contamination of some illite separates by low-K material, most plausibly smectite of detrital origin. There is no correlation between K-content and the burial depth at the time of illite formation, suggesting that a process is operating that alters the illite composition after initial formation.

(2) The K-contents of the illite is consistent with the fundamental particle model, with increasing particle thickness as temperature increases. To reconcile measured K-contents with theoretical values, there must be hydronium ions within the interlayer sites of the illite. There is independent

evidence for this in the form of measured structural water contents in illite samples, the majority of which exceed the theoretical value of the fundamental particle model. The measured thicknesses of fundamental particles are consistent with a published theoretical model of continuous illite nucleation and growth, again suggesting alteration after initial formation.

(3) Crystal ripening is identified as the most probable process of post-formation alteration of the illite fundamental particles. The degree to which argon is expelled from the illite during dissolution and growth is unknown, but may be largely retained (75−100%), as has been suggested for the smectite to illite transformation in shales.

ACKNOWLEDGMENTS

REFERENCES

Aja S.U. (1995) Thermodynamic properties of some 2:1 layer clay minerals from solution equilibration data. *European Journal of Mineralogy*, **7**, 325−333.

Baronnet A. (1982) Ostwald ripening in solution: the case of calcite and mica. *Estudios Geológicos*, **38**, 185−198.

Bauer A., Velde B. & Gaupp R. (2000) Experimental constraints on illite crystal morphology. *Clay Minerals*, **35**, 587−597.

Burley S.D. & Flisch M. (1989) K−Ar geochronology and the timing of detrital I/S clay illitization and authigenic illite precipitation in the Piper and Tartan Fields, Outer Moray Firth, UK North Sea. *Clay Minerals*, **24**, 285−315.

Clauer N., Rinckenbach T., Weber F., Sommer F., Chaudhuri S. & O'Neil J.R. (1999) Diagenetic evolution of clay minerals in oil-bearing neogene sandstones and associated shales, Mahakam Delta Basin, Kalimantan, Indonesia. *American Association of Petroleum Geologists Bulletin*, **83**, 62−87.

Darby D., Wilkinson M., Haszeldine R.S. & Fallick A.E. (1997) Illite dates record deep fluid movements in petroleum basins. *Petroleum Geoscience*, **3**, 133−140.

Deer W.A., Howie R.A. & Zussman J. (1966) *An Introduction to the Rock Forming Minerals*. Longman Group Limited, Harlow, England, 528 pp.

Drits V.A. & McCarty D.K. (2010) The nature of structure-bonded H_2O in illite and leucophyllite from dehydration and dehydroxylation experiments. *Clays and Clay Minerals*, **55**, 45−58.

Eberl D.D. & Środoń J. (1988) Ostwald ripening and interparticle-diffraction effects for illite crystals. *American Mineralogist*, **73**, 1335−1345.

Ehrenberg S.N. & Nadeau P.H. (1989) Formation of diagenetic illite in sandstones of the Garn Formation, Haltenbanken area, mid−Norwegian continental shelf. *Clay Minerals*, **24**, 233−253.

Egeberg P.K. & Aagaard P. (1989) Origins and evolution of formation waters from oil fields on the Norwegian Shelf. *Applied Geochemistry*, **4**, 131−142.

Fallick A.E., Macaulay C.I. & Haszeldine R.S. (1993) Implications of linearly correlated oxygen and hydrogen isotopic compositions for kaolinite and illite in the Magnus Sandstone, North Sea. *Clays and Clay Minerals*, **41**, 184−190.

Giles M.R., Stevenson S., Martin S.V., Cannon S.J.C., Hamilton P.J., Marshall J.D. & Samways G.M. (1992) The reservoir properties and diagenesis of the Brent Group: a regional perspective. Pp. 289−327 in: *Geology of the Brent Group* (A.C. Morton, R.S. Haszeldine, M.R. Giles & S. Brown, editors). Geological Society London. Special Publication, **61**.

Girard J.P., Munz I.A., Johansen H., Lacharpagne J.C. & Sommer F. (2002) Diagenesis of the Hild Brent sandstones, northern North Sea: isotopic evidence for the prevailing influence of deep basinal water. *Journal of Sedimentary Research*, **72**, 746−759.

Glasmann J.R., Clark R.A., Larter S., Briedis N.A. & Lundegard P.D. (1989) Diagenesis and hydrocarbon accumulation, Brent Sandstone (Jurassic), Bergen High area, North Sea. *American Association of Petroleum Geologists Bulletin*, **73**, 1341−1360.

Greenwood P.J., Shaw H.F. & Fallick A.E. (1994) Petrographic and isotopic evidence for diagenetic processes in Middle Jurassic sandstones and mudrocks from the Brae area, North Sea. *Clay Minerals*, **29**, 637−650.

Hamilton P.J., Giles M.R. & Ainsworth, P. (1992) K−Ar dating of illites in Brent Group reservoirs: a regional perspective. Pp. 377−400 in: *Geology of the Brent Group* (A.C. Morton, R.S. Haszeldine, M.R. Giles & S. Brown, editors). Geological Society London. Special Publication, **61**.

Hamilton P.J., Kelley S. & Fallick A.E. (1989) K-Ar dating of illite in hydrocarbon reservoirs. *Clay Minerals*, **24**, 215−232.

Hogg A.J.C., Hamilton P.H. & Mcintyre (1993) Mapping diagenetic fluid flow within a reservoir: K-Ar dating in the Alwyn area (UK North Sea).

Marine and Petroleum Geology, **10**, 279−294.

Jiang W.T., Peacor D.R. & Essene E.J. (1994) Clay minerals in the Macadams Sandstone, California; implications for substitution of H_3O^+ and H_2O and metastability of illite. *Clays and Clay Minerals*, **42**, 35−45.

Kang I.-M., Hillier S., Song Y. & Kim I.-J. (2012) Relative coherent stacking potential of fundamental particles of illite-smectite and its relationship to geological environment. *Clay Minerals*, **47**, 319−327.

Lander R.H. & Bonnell L.M. (2010) A model for fibrous illite nucleation and growth in sandstones. *American Association of Petroleum Geologists Bulletin*, **94**, 1161−1187.

Lanson B. & Champion D. (1991) The I/S-to-illite reaction in the late stage diagenesis. American Journal of Science, **29l**, 473−506.

Lasocki J., Guememe J.M., Hedayati A., Legorjus C. & Page W.M. (1999) The Elgin and Franklin fields: UK Blocks 22/30c, 22/30-b and 29/5b. Pp. 1007−1020 in: *Petroleum Geology of Northwest Europe: Proceedings of the 5th Conference* (A. Fleet & S.A.R. Boldy, editors). Geological Society, London.

Leveille G.P., Primmer T.J., Dudley G., Ellis D. & Allinson G.J. (1997) Diagenetic controls on reservoir quality in Permian Rotliegendes sandstones, Jupiter Fields area, southern North Sea. Pp. 105−122 in: *Petroleum Geology of the Southern North Sea: Future Potential* (K. Zeigler, P. Turner & S.R. Daines, editors). Geological Society Special Publication, **123**.

Liewig N. & Clauer N. (2000) K-Ar dating of varied microtextural illite in Permian gas reservoirs, northern Germany. *Clay Minerals*, **35**, 271−281.

McBride J.J. (1992) *The Diagenesis of Middle Jurassic Reservoir Sandstones of Bruce Field, UK North Sea*. PhD thesis, University of Aberdeen.

Macaulay C.I., Haszeldine R.S. & Fallick A.E. (1992) Diagenetic pore waters stratified for at least 35 million years – Magnus Oil-Field, North-Sea. *American Association of Petroleum Geologists Bulletin*, **76**, 1625−1634.

Matthews J.C., Velde B. & Johansen H. (1994) Significance of K−Ar ages of authigenic illitic clay−minerals in sandstones and shales from the North Sea. *Clay Minerals*, **29**, 379−389.

Morton A., Hallsworth C., Strogen D., Whitham A. & Fanning M. (2009) Evolution of provenance in the NE Atlantic rift: The Early−Middle Jurassic succession in the Heidrun field, Halten Terrace, offshore Mid-Norway. *Marine and Petroleum Geology*, **26**, 1100−1117.

Mullin J.W. (1961) *Crystallization*. Butterworth-Heinemann, Oxford.

Nadeau P.H. (1985) The physical dimensions of fundamental clay particles. *Clay Minerals*, **20**, 499−514.

Nadeau P.H. (1987) Relationships between the mean area, volume and thickness for dispersed particles of kaolinites and miceaceous clays and their application to surface area and ion exchange properties. *Clay Minerals*, **22**, 351−356.

Neuman A.C.D. and Brown G. (1987) The chemical constitution of clays. Pp. 1−128 in: *Chemistry of Clays and Clay Minerals* (A.C.D. Neuman, editor). Mineralogical Society Monograph, **6**, 480 pp.

Nieto F., Mellini F. & Abad I. (2010) The role of H_3O^+ in the crystal structure of illite. *Clays and Clay Minerals*, **58**, 238−246.

Primmer T.J., Warren E.A., Sharma B.K. & Atkins (1993) The stability of experimentally grown clay minerals: implications for modelling the stability of neo-formed diagenetic clay minerals. Pp. 163−180 in: *Geochemistry of Clay–Pore Fluid Interactions* (D.A.C. Manning, P.L. Hall & C.R. Hughes). Chapman and Hall, London, 427 pp.

Vidal O., Dubacq B. & Lanari P. (2010) Comment on "The role of H_3O^+ in the crystal structure of illite" by F. Nieto, M. Melini, and I. Abad. *Clays and Clay Minerals*, **58**, 717−720.

Warren E.A. & Smalley P.C. (1994) *North Sea Formation Waters Atlas*. Geological Society, London, Memoir 11.

Wilkinson M. & Haszeldine R.S. (2002a) Fibrous illite in oilfield sandstones − a nucleation kinetic theory of growth. *Terra Nova*, **14**, 56−60.

Wilkinson M. & Haszeldine R.S. (2002b) Problems with argon: K−Ar ages in Gulf Coast shales. *Chemical Geology*, **191**, 277−283.

Wilkinson, M. & Haszeldine, R.S. (2011) Oil charge preserves exceptional porosity in deeply buried, overpressured, sandstones: Central North Sea, UK. *Journal of the Geological Society*, **168**, 1285−1295.

Wilkinson M., Fallick A.E., Keaney G.M.J., Haszeldine R.S. & McHardy W. (1994) Stable isotopes in illite: the case for meteoric water flushing within the Upper Jurassic Fulmar Formation sandstones, UK North Sea. *Clay Minerals*, **29**, 567−574.

Wilkinson M., Haszeldine R.S. & Fallick A.E. (2006) Jurassic and Cretaceous clays of the northern and central North Sea: Hydrocarbon reservoirs reviewed. *Clay Minerals*, **41**, 151−186.

Yates D.M. & Rosenberg P.E. (1998) Characterization of neoformed illite from hydrothermal experiments at 250ºC and $P_{v, soln}$: An HRTEM/ATEM study. *American Mineralogist*, **83**, 1199−1208.

Ziegler K., Sellwood B.W. & Fallick A.E. (1994) Radiogenic and stable isotope evidence for age and origin of authigenic illites in the Rotliegend, southern North Sea. *Clay Minerals*, **29**, 555−565.